



# Effect of rare-earth dopants on the thermal behavior of tungsten–tellurite glasses

A.E. Ersundu\*, G. Karaduman, M. Çelikbilek, N. Solak, S. Aydın

Istanbul Technical University, Department of Metallurgical and Materials Engineering, Istanbul, 34469, Turkey

## ARTICLE INFO

### Article history:

Received 18 June 2010

Received in revised form 25 August 2010

Accepted 25 August 2010

### Keywords:

Amorphous materials

Rare-earth alloys and compounds

Rapid-solidification

Quenching

Thermodynamic properties

Thermal analysis

## ABSTRACT

In the present study, the effect of rare-earth element addition on the thermal behavior of tungsten–tellurite glasses was investigated by running detailed differential thermal analyses. The glasses were prepared with the compositions of  $(1-x)\text{TeO}_2-x\text{WO}_3$ , where  $x=0.10, 0.15$  and  $0.20$  in molar ratio and all three samples were doped with  $0.5$  and  $1.0$  mol% of  $\text{Nd}_2\text{O}_3$ ,  $\text{Er}_2\text{O}_3$ ,  $\text{Tm}_2\text{O}_3$  and  $\text{Yb}_2\text{O}_3$ . By applying different glass preparing methods, the effect of melt-quenching techniques on the thermal behavior of tellurite glasses was also investigated and almost the same thermal behavior was observed for all attempts. Therefore, the glass samples were obtained by heating high purity powder mixtures to  $800^\circ\text{C}$  in a platinum crucible with a closed lid, holding for  $30$  min and quenching in water bath. In general, the addition of rare-earth elements to undoped samples affected the thermal behavior of tungsten–tellurite glasses by shifting the glass transition and exothermic reaction temperatures to higher values and increasing the thermal stability. Moreover, the introduction of rare-earth dopants significantly decreased the temperature values of the first endothermic peaks corresponding to the eutectic reaction; whereas a slight decrease was observed in the second endothermic peak temperatures representing the liquidus reaction. Addition of rare-earth elements with higher atomic number ( $\text{Er}_2\text{O}_3$ ,  $\text{Tm}_2\text{O}_3$  and  $\text{Yb}_2\text{O}_3$ ) resulted in peak splitting of the eutectic reaction.

© 2010 Elsevier B.V. All rights reserved.

## 1. Introduction

Tellurite glasses have received considerable attention for their potential use in fiber optics, laser hosts and non-linear optical materials. Tellurium oxide, as a pure oxide, does not have glass forming ability under normal cooling conditions, therefore addition of a network modifier such as heavy metal oxides ( $\text{PbO}$ ,  $\text{Bi}_2\text{O}_3$  and  $\text{WO}_3$  etc.) increase the glass forming ability. Among heavy metal oxide containing tellurite glasses, tungsten–tellurite glasses exhibit various excellent properties such as doping in a wide range, modifying the composition by a third, fourth, and even fifth component which allows controlling the optical properties, enhancing the chemical stability and devitrification resistance [1–4]. It is known that the main drawbacks of tellurite glasses are their low glass transition temperature and relatively low-phonon energy. However, since tungsten–tellurite glasses have slightly higher phonon energy and higher glass transition temperature compared to other tellurite glasses, they can be used at high optical intensities without exposure to thermal damage [5].

Glasses doped with rare-earth ions have been investigated intensively for fabricating lasers and amplifiers since the last quarter of the twentieth century. Tellurite glasses doped with rare-earth ions have attracted a great deal of interest due to their advanta-

geous properties over silicate, borate and phosphate glasses such as a wide transmission range from ultraviolet to mid-infrared, low-phonon energy, high refractive index, high dielectric constant and chemical stability [1–3,6–10]. The optical properties of different rare-earth element ions in tellurite based systems have been extensively studied for several years.  $\text{Nd}^{3+}$ ,  $\text{Er}^{3+}$ ,  $\text{Tm}^{3+}$  and  $\text{Yb}^{3+}$  are the most commonly used rare-earth ions in tungsten–tellurite glasses.  $\text{Er}^{3+}$  and  $\text{Tm}^{3+}$  doped tellurite glasses find wide applications which involve  $\text{Er}^{3+}$  doped fiber amplifiers (EDFA) for C and L bands and  $\text{Tm}^{3+}$  doped fiber amplifiers (TDFA) for the S band [5,11]. Moreover,  $\text{Nd}^{3+}$  doped tellurite glasses show efficient laser emission closer to Q-switched operation under pulsed excitation and  $\text{Yb}^{3+}$  doped tellurite glasses are advantageous for Q-switched lasers, high power ultra short pulse amplification and also for sensitizers of energy transfer [12,13].

There exists a substantial amount of literature on the optical properties of  $\text{Nd}^{3+}$ ,  $\text{Er}^{3+}$ ,  $\text{Tm}^{3+}$  and  $\text{Yb}^{3+}$  doped tungsten–tellurite glasses [14–20]. However, apart from the study realized by El-Mallawany and Abbas Ahmed [21] which reported the effect of  $\text{Nd}^{3+}$  and  $\text{Er}^{3+}$  on the glass transition temperature of tellurite based quaternary glasses, no studies exist about the effect of rare-earth elements on the thermal behavior of tellurite glasses in a wide temperature range. Therefore, in the present study, we report, for the first time to our knowledge, the effect of rare-earth oxides ( $\text{Nd}_2\text{O}_3$ ,  $\text{Er}_2\text{O}_3$ ,  $\text{Tm}_2\text{O}_3$  and  $\text{Yb}_2\text{O}_3$ ) on the thermal behavior of tellurite glasses by running detailed differential thermal analyses. Since different glass preparing methods are used in the literature to obtain

\* Corresponding author. Tel.: +90 212 285 7203; fax: +90 212 285 3427.  
E-mail address: [ersundu@itu.edu.tr](mailto:ersundu@itu.edu.tr) (A.E. Ersundu).

**Table 1**

Labels of the doped samples and change in glass composition with respect to subtraction of rare-earth oxide addition from different components in the glass system.

| (1-x)TeO <sub>2</sub> -xWO <sub>3</sub> | Rare-earth dopant content (mol%) | Label      | Subtraction from TeO <sub>2</sub> |                     | Subtraction from WO <sub>3</sub> |                     | Subtraction from both TeO <sub>2</sub> and WO <sub>3</sub> |                     |
|---|----------------------------------|------------|-----------------------------------|---------------------|----------------------------------|---------------------|--|---------------------|
|   |                                  |            | TeO <sub>2</sub> (%)              | WO <sub>3</sub> (%) | TeO <sub>2</sub> (%)             | WO <sub>3</sub> (%) | TeO <sub>2</sub> (%)                                       | WO <sub>3</sub> (%) |
| x = 0.10<br>(TW10)                      | 0.5                              | TW10-RE0.5 | 89.5                              | 10                  | 90                               | 9.5                 | 89.55  | 9.95                |
|   | 1.0                              | TW10-RE1.0 | 89                                | 10                  | 90                               | 9                   | 89.1   | 9.9                 |
| x = 0.15<br>(TW15)                      | 0.5                              | TW15-RE0.5 | 84.5                              | 15                  | 85                               | 14.5                | 84.575   | 14.925              |
|   | 1.0                              | TW15-RE1.0 | 84                                | 15                  | 85                               | 14                  | 84.15  | 14.85               |
| x = 0.20<br>(TW20)                      | 0.5                              | TW20-RE0.5 | 79.5                              | 20                  | 80                               | 19.5                | 79.6   | 19.9                |
|   | 1.0                              | TW20-RE1.0 | 79                                | 20                  | 80                               | 19                  | 79.2   | 19.8                |

RE (Nd<sub>2</sub>O<sub>3</sub>, Er<sub>2</sub>O<sub>3</sub>, Tm<sub>2</sub>O<sub>3</sub>, Yb<sub>2</sub>O<sub>3</sub>).

tellurite glasses with better optical properties, in the present study the effect of different melt-quenching techniques on the thermal behavior of tellurite glasses was also investigated.

## 2. Experimental procedure

From the glass forming region of TeO<sub>2</sub>-WO<sub>3</sub> system, three compositions were selected for the present investigation on the basis of the knowledge obtained from our earlier studies on tungsten-tellurite binary system due to their high glass forming ability and chemical stability [2,4,7,8,22–25]. Therefore, different glass samples were prepared with the compositions of (1-x)TeO<sub>2</sub>-xWO<sub>3</sub>, where x = 0.10, 0.15 and 0.20 in molar ratio, and the samples were named as TW10, TW15 and TW20, respectively. According to these compositions, all three samples were doped with 0.5 and 1.0 mol% of Nd<sub>2</sub>O<sub>3</sub>, Er<sub>2</sub>O<sub>3</sub>, Tm<sub>2</sub>O<sub>3</sub> and Yb<sub>2</sub>O<sub>3</sub> to investigate the effect of rare-earth dopants on the thermal behavior of tungsten-tellurite glasses. Table 1 presents the labels of the doped samples and the compositional change in tungsten-tellurite glasses with respect to subtraction of rare-earth oxide addition from different components.

There exist different approaches for rare-earth doping in tungsten-tellurite glasses such as, subtraction of rare-earth dopant addition from the glass former (TeO<sub>2</sub>), from the network modifier (WO<sub>3</sub>) or both from the glass former and network modifier. Although, the changes in the glass composition are very small as a result of different subtraction approaches, the stoichiometry of the glasses change by subtracting rare-earth dopant addition only from one component in the glass system. Therefore, in the present study rare-earth doping was realized by subtracting rare-earth oxide addition from both TeO<sub>2</sub> and WO<sub>3</sub> in order to keep the stoichiometry of the glasses constant.

To investigate the effect of rare-earth dopants on the thermal behavior, the glass samples were prepared by applying a conventional melt-quenching technique using reagent-grade powders of TeO<sub>2</sub> (99.99% purity, Alfa Aesar Company), WO<sub>3</sub> (99.8% purity, Alfa Aesar Company), Nd<sub>2</sub>O<sub>3</sub> (99.9% purity, Alfa Aesar Company), Er<sub>2</sub>O<sub>3</sub> (99.9% purity, Sigma-Aldrich Company), Tm<sub>2</sub>O<sub>3</sub> (99.99% purity, Sigma-Aldrich Company) and Yb<sub>2</sub>O<sub>3</sub> (99.9% purity, Alfa Aesar Company). The powder batches of 2 g size were thoroughly mixed in an agate mortar and melted in a platinum crucible with a closed lid at 800 °C for 30 min to provide complete homogeneity of the melts and then the molten samples were removed from the furnace and quenched in water bath.

Different glass preparing methods were applied in the literature to acquire tellurite glasses with better optical properties, therefore the effect of different glass preparing techniques on the thermal behavior was investigated and for this purpose 1.0 mol% Tm<sub>2</sub>O<sub>3</sub> doped TW20 sample was prepared via three different melt-quenching techniques. As the first glass preparing method, the powder batches were melted in a platinum crucible with a closed lid at 800 °C for 30 min, removed from the furnace and quenched in water bath which was also used for the investigation of the effect of rare-earth dopants on the thermal behavior. As the second glass preparing method, the powder batches were melted at the same temperature for 30 min and quenched in water bath and then crushed and powdered to achieve homogenization. Afterwards, the powdered sample was re-melted and quenched in water bath. Lastly, as the third glass preparing method, the same melting procedure was applied and the glass melts were casted into a pre-heated stainless steel mold.

The thermal characterization experiments were realized by using differential thermal analysis (DTA) technique. DTA scans of the samples were carried out in a PerkinElmer™ Diamond TG/DTA to determine the glass transition onset (*T<sub>g</sub>*), crystallization onset and peak (*T<sub>c</sub>*/*T<sub>p</sub>*), melting onset and peak (*T<sub>mo</sub>*/*T<sub>mp</sub>*) temperatures. The temperature difference between the *T<sub>g</sub>* and the first exothermic peak onset (*T<sub>c1</sub>*),  $\Delta T = T_{c1} - T_g$ , indicating the thermal stability against crystallization was calculated. The glass transition onset temperatures (*T<sub>g</sub>*) were determined as the inflection point of the endothermic change of the calorimetric signal. Onset temperatures were specified as the beginning of the reaction where the crystallization or melting first starts and peak temperatures represent the maximum value of the exotherm or endotherm. The DTA scans were recorded by using 25 mg powdered samples. All

thermal analyses were realized in a platinum crucible with a heating rate of 10 K/min from room temperature to 750 °C in a flowing (100 ml/min) argon gas.

## 3. Results and discussion

### 3.1. Effect of glass preparing methods on the thermal behavior

The DTA curves of 1.0 mol% Tm<sub>2</sub>O<sub>3</sub> doped TW20 samples prepared via three different methods are given in Fig. 1.

As can be seen from Fig. 1, almost the same thermal behavior was observed for all three samples prepared via different melt-quenching techniques. However, the prepared glasses with different methods showed different colors representing a change in their optical properties. Therefore, it can be concluded that although different glass preparing techniques affect the optical properties, they do not have a significant effect on the thermal behavior. Since the thermal behavior of the glasses are not affected due to different glass preparing methods, in the experimental studies all the samples were prepared by applying the first glass preparing method (melting and quenching in water bath).

### 3.2. Effect of rare-earth dopants on the thermal behavior

The DTA curves of undoped and 0.5–1.0 mol% rare-earth oxide (Nd<sub>2</sub>O<sub>3</sub>, Er<sub>2</sub>O<sub>3</sub>, Tm<sub>2</sub>O<sub>3</sub> and Yb<sub>2</sub>O<sub>3</sub>) doped TW10, TW15 and TW20 glasses are shown in Fig. 2, Fig. 3 and Fig. 4, respectively. In general, the DTA curves showed a glass transition, several exothermic peaks

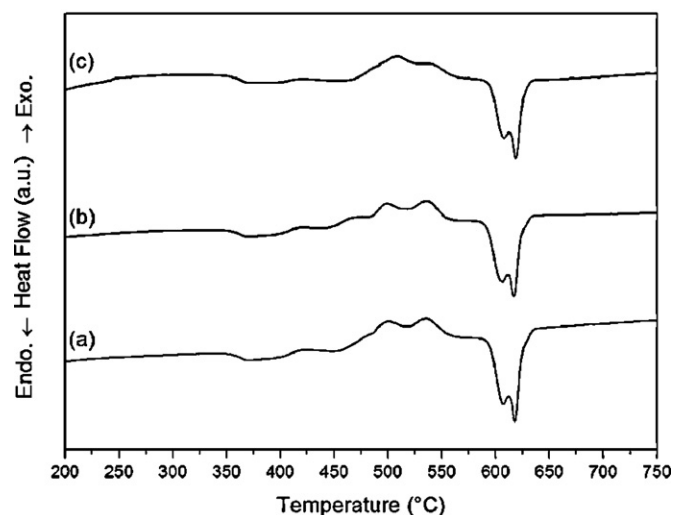


**Fig. 1.** Effect of different glass preparing methods on the thermal behavior of 1.0 mol% Tm<sub>2</sub>O<sub>3</sub> doped TW20 sample, (a) melted and quenched in water bath, (b) melted and quenched in water bath, to achieve homogenization crushed and powdered, re-melted and quenched in water bath, (c) melted and casted into a pre-heated stainless steel mold.

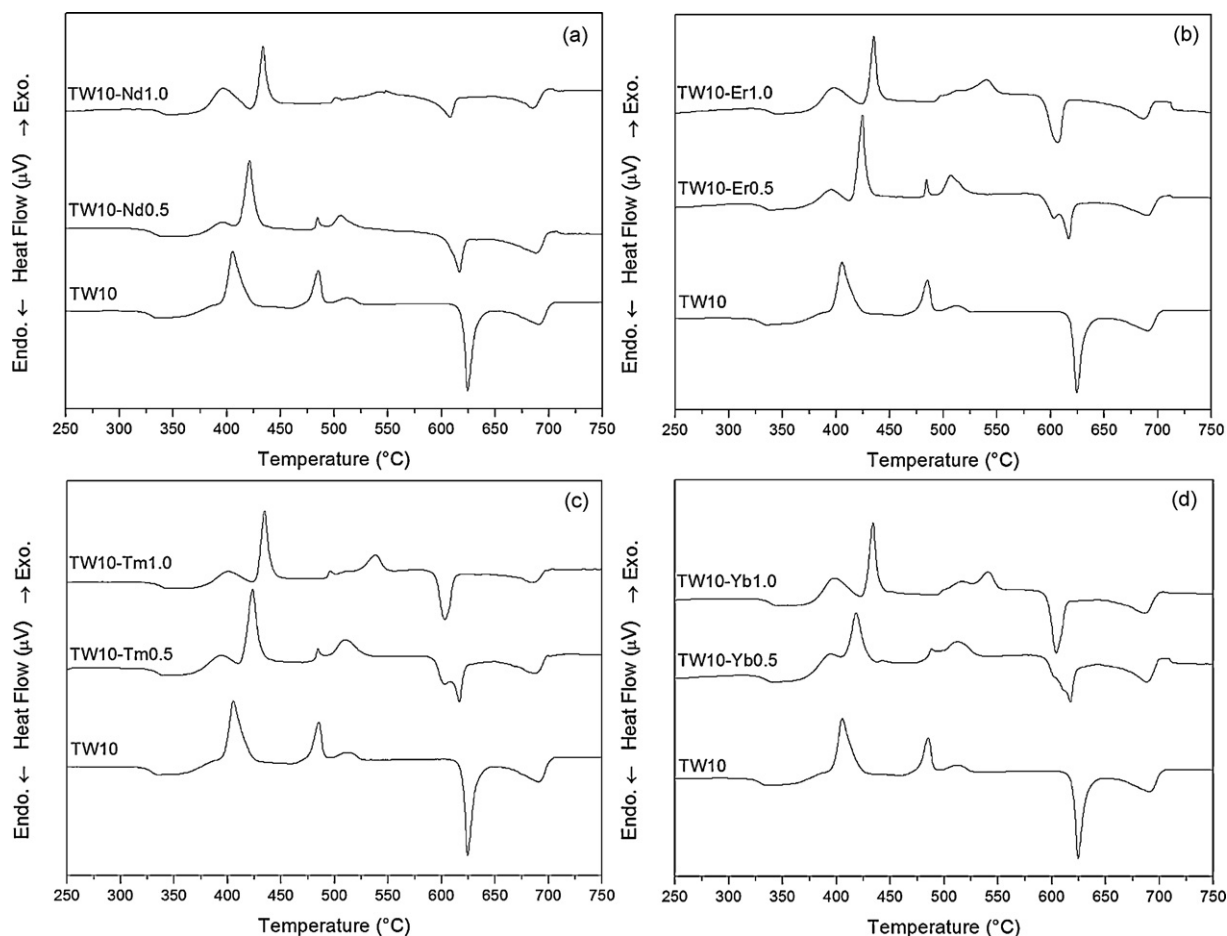


Fig. 2. DTA curves of undoped and 0.5–1.0 mol% (a)  $\text{Nd}_2\text{O}_3$ , (b)  $\text{Er}_2\text{O}_3$ , (c)  $\text{Tm}_2\text{O}_3$  and (d)  $\text{Yb}_2\text{O}_3$  doped TW10 glass

Table 2

Values of glass transition onset,  $T_g$ , crystallization onset and peak,  $T_c/T_p$ , melting onset and peak,  $T_{m0}/T_{mp}$  temperatures of the undoped and rare-earth oxide doped TW10, TW15 and TW20 glasses.

| Label      | $T_g$ (°C) | $T_{c1}/T_{p1}$ (°C) | $T_{c2}/T_{p2}$ (°C) | $T_{c3}/T_{p3}$ (°C) | $T_{c4}/T_{p4}$ (°C) | $T_{m01}/T_{mp1}$ -(a) (°C) | $T_{m01}/T_{mp1}$ -(b) (°C) | $T_{m02}/T_{mp2}$ (°C) |
|------------|------------|----------------------|----------------------|----------------------|----------------------|-----------------------------|-----------------------------|------------------------|
| TW10       | 321        | 363/–                | –/405                | 476/485              | –/512                |                             | 619/624                     | –/691                  |
| TW10–Nd0.5 | 324        | 374/396              | –/421                | 482/484              | 498/506              |                             | 602/617                     | –/688                  |
| TW10–Er0.5 | 327        | 376/396              | –/424                | 482/484              | 498/507              | 592/603                     | –/617                       | –/690                  |
| TW10–Tm0.5 | 327        | 371/394              | –/423                | 480/485              | 498/510              | 593/603                     | –/616                       | –/696                  |
| TW10–Yb0.5 | 327        | 375/394              | –/418                | 482/489              | –/513                | 594/–                       | –/617                       | –/688                  |
| TW10–Nd1.0 | 332        | 378/396              | –/434                | 497/502              | –/544                |                             | 601/608                     | –/685                  |
| TW10–Er1.0 | 330        | 378/398              | –/435                | 493/497              | 525/540              |                             | 593/607                     | –/687                  |
| TW10–Tm1.0 | 331        | 379/401              | 428/435              | 492/496              | 524/538              |                             | 595/603                     | –/685                  |
| TW10–Yb1.0 | 331        | 380/398              | –/434                | –/517                | –/541                |                             | 596/604                     | –/686                  |
| TW15       | 335        | 414/433              | –/471                | –/481                | –/502                |                             | 619/625                     | –/662                  |
| TW15–Nd0.5 | 339        | 418/439              | –/483                | –/508                |                      |                             | 604/621                     | –/660                  |
| TW15–Er0.5 | 338        | 428/447              | –/483                | –/502                |                      | 590/603                     | –/620                       | –/661                  |
| TW15–Tm0.5 | 337        | 426/443              | –/481                | –/500                |                      | 590/–                       | –/619                       | –/659                  |
| TW15–Yb0.5 | 337        | 420/441              | –/484                | –/502                |                      | 598/–                       | –/620                       | –/664                  |
| TW15–Nd1.0 | 342        | 421/445              | –/497                | –/523                |                      |                             | 597/610                     | –/656                  |
| TW15–Er1.0 | 343        | 435/454              | –/496                | –/523                |                      | 592/606                     | –/615                       | –/658                  |
| TW15–Tm1.0 | 341        | 431/449              | –/496                | –/520                |                      | 593/604                     | –/611                       | –/658                  |
| TW15–Yb1.0 | 344        | 428/452              | –/498                | –/523                |                      | 595/604                     | –/611                       | –/657                  |
| TW20       | 344        | 439/–                | –/481                | –/508                |                      |                             | 620/626                     |                        |
| TW20–Nd0.5 | 351        | 445/–                | –/490                | –/523                |                      |                             | 602/622                     |                        |
| TW20–Er0.5 | 349        | –/471                | –/492                | –/520                |                      | 592/604                     | –/622                       |                        |
| TW20–Tm0.5 | 349        | 446/471              | –/493                | –/523                |                      | 591/–                       | –/622                       |                        |
| TW20–Yb0.5 | 347        | 446/–                | –/488                | –/523                |                      | 593/–                       | –/622                       |                        |
| TW20–Nd1.0 | 354        | 442/476              | –/494                | –/534                |                      |                             | 604/618                     |                        |
| TW20–Er1.0 | 350        | 455/482              | –/506                | –/534                |                      | 590/605                     | –/617                       |                        |
| TW20–Tm1.0 | 354        | 455/–                | –/501                | –/535                |                      | 595/607                     | –/618                       |                        |
| TW20–Yb1.0 | 354        | 446/–                | –/498                | –/533                |                      | 597/607                     | –/618                       |                        |

– ;Undetermined values.

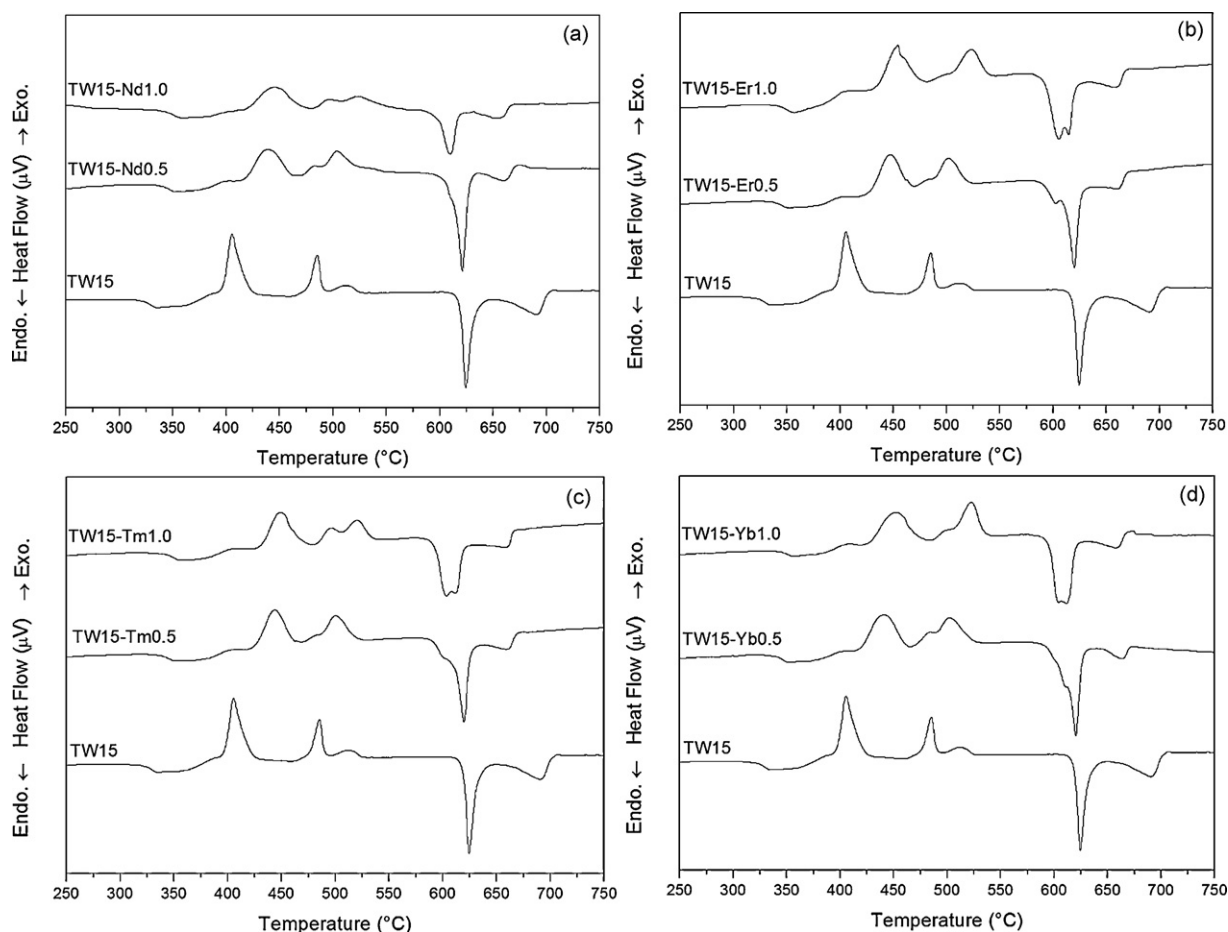


Fig. 3. DTA curves of undoped and 0.5–1.0 mol% (a)  $\text{Nd}_2\text{O}_3$ , (b)  $\text{Er}_2\text{O}_3$ , (c)  $\text{Tm}_2\text{O}_3$  and (d)  $\text{Yb}_2\text{O}_3$  doped TW15 glass

related to the crystallization and transformation of different crystalline phases and endothermic peaks corresponding to the melting of the existing phases. The details of thermal analyses are listed in Table 2.

A shallow broad endothermic change of the calorimetric signal corresponding to the glass transition temperature ( $T_g$ ) was observed for all DTA scans indicating the glassy nature of the samples. For undoped TW10, TW15 and TW20 samples, the glass transition onset temperatures were specified at 321, 335 and 344 °C, respectively; whereas for rare-earth oxide doped samples the glass transition onset temperatures were detected at higher temperatures.

The crystallization onset and peak temperatures were also determined at higher values for rare-earth oxide doped samples than the undoped samples (see Table 2). Introducing rare-earth elements into undoped tellurite glasses and increasing their content from 0.5 to 1.0 mol% shifted the crystallization onset and peak temperatures to higher values. There exists no information in the literature about the effect of rare-earth dopants on the crystallization temperatures. However, since a similar behavior was observed for glass transition and crystallization reactions, it can be concluded that introducing rare-earth elements into tellurite glasses and increasing their content resulted in an increase in both glass transition and crystallization temperatures, which was probably due to the increase in number of bonds per unit volume as also reported by El-Mallawany and Abbas Ahmed [21] for glass transition temperature.

As can be seen from Figs. 2 and 3, two endothermic peaks were detected for TW10 and TW15 samples; whereas TW20 sam-

ple showed only one endothermic peak (see Fig. 4). The first endothermic onset temperatures were determined at  $619 \pm 1$  °C for all undoped samples corresponding to the binary eutectic reaction: liquid  $\rightarrow \alpha\text{-TeO}_2 + \text{WO}_3$  of the  $\text{TeO}_2\text{--WO}_3$  system which was reported in the literature by several researchers [3,4,23–26]. The second endothermic peaks observed in TW10 and TW15 samples were attributed to the liquidus reaction of the binary system [23–25]. However, since the TW20 sample is very close to the eutectic composition determined by Blanchandin et al. [4] as  $22 \pm 1$  mol%  $\text{WO}_3$ , only one endothermic peak was observed in the DTA scans.

Introducing rare-earth elements ( $\text{Nd}_2\text{O}_3$ ,  $\text{Er}_2\text{O}_3$ ,  $\text{Tm}_2\text{O}_3$  and  $\text{Yb}_2\text{O}_3$ ) into the undoped glasses resulted in a change in the melting behavior (see Figs. 2–4). In general, addition of 0.5 mol% content of rare-earth oxides significantly decreased the temperature values of the first endothermic peaks corresponding to the eutectic reaction however caused a slight decrease on the second endothermic peak temperatures related to the liquidus reaction. Increasing the rare-earth dopant content to 1.0 mol% shifted the eutectic reaction temperatures to much lower values; however a slight shift to lower temperature values was observed for liquidus reaction. In the literature, Zhang and Poulain [27] reported that there is a 2/3 ratio between the glass transition and liquidus temperatures and since the addition of rare-earth fluorides with higher melting point increase the glass transition temperature of the fluorogallate glasses, the liquidus temperature also increase with the rare-earth addition. However, in the present study it can be clearly seen that the addition of rare-earth elements decrease the melting temperature of the glass samples.

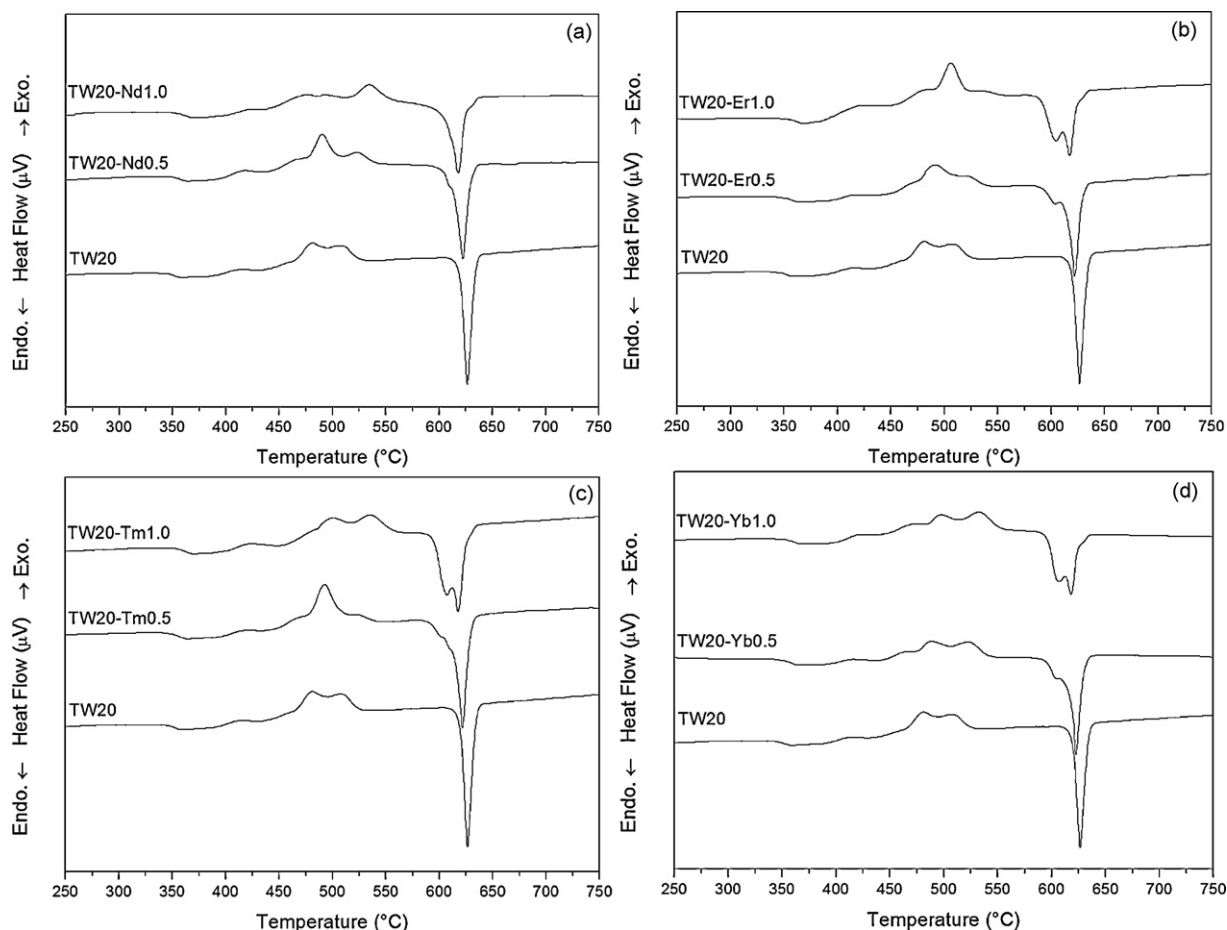


Fig. 4. DTA curves of undoped and 0.5–1.0 mol% (a)  $\text{Nd}_2\text{O}_3$ , (b)  $\text{Er}_2\text{O}_3$ , (c)  $\text{Tm}_2\text{O}_3$  and (d)  $\text{Yb}_2\text{O}_3$  doped TW20 glass.

Addition of  $\text{Er}_2\text{O}_3$ ,  $\text{Tm}_2\text{O}_3$  and  $\text{Yb}_2\text{O}_3$  caused the splitting of the first endothermic peak corresponding to the eutectic reaction into two peaks which was not observed in  $\text{Nd}_2\text{O}_3$  addition. This was probably due to the higher atomic number of the  $\text{Er}_2\text{O}_3$ ,  $\text{Tm}_2\text{O}_3$  and  $\text{Yb}_2\text{O}_3$  compared to  $\text{Nd}_2\text{O}_3$ , since the ionic radius of the rare-earth oxides decreases with the increasing atomic number due to the rare-earth contraction and the glass network becomes more compact which leads to an increase of the density [28].

In the literature, a similar behavior of peak splitting was observed by Öveçoğlu et al. [3] for the first endothermic peak corresponding to the eutectic reaction in 1.0 mol%  $\text{Tm}_2\text{O}_3$  containing TW15 glass. However, they reported that identical DTA curves were obtained for undoped and 1.0 mol%  $\text{Tm}_2\text{O}_3$  doped samples. Moreover, in their study the endothermic peak detected at lower temperatures was thought to be due to the melting reaction of a metastable phase. However, in the present study it can be clearly seen that the addition of rare-earth dopants with higher atomic number ( $\text{Er}_2\text{O}_3$ ,  $\text{Tm}_2\text{O}_3$ ,  $\text{Yb}_2\text{O}_3$ ) resulted in peak splitting of the first endothermic reaction and shifted the peak temperatures to lower values. This can be explained as the addition of the rare-earth dopant acts as a third component in the glass system and results a change in the binary equilibria of the system to a ternary equilibria.

### 3.3. Effect of rare-earth dopants on the glass transition temperature and thermal stability

The effect of rare-earth dopants ( $\text{Nd}_2\text{O}_3$ ,  $\text{Er}_2\text{O}_3$ ,  $\text{Tm}_2\text{O}_3$  and  $\text{Yb}_2\text{O}_3$  mol%) on glass transition temperature is shown in Fig. 5.

For all the samples, the addition of 0.5 mol% content of rare-earth elements increased the glass transition temperatures. By increasing the rare-earth element content from 0.5 to 1.0 mol% the glass transition temperatures were shifted to much higher values. With the addition of rare-earth elements into undoped tellurite glasses and increasing their content, the glass transition temperatures increased from 321 to 332 °C for TW10, 335 to 344 °C for TW15 and 344 to 354 °C for TW20 glasses. Therefore, it can be concluded that

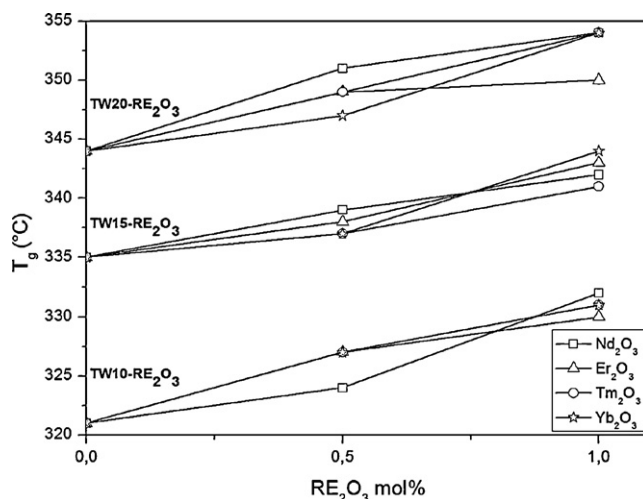


Fig. 5. Effect of rare-earth dopants ( $\text{Nd}_2\text{O}_3$ ,  $\text{Er}_2\text{O}_3$ ,  $\text{Tm}_2\text{O}_3$ ,  $\text{Yb}_2\text{O}_3$  mol%) on glass transition temperature of TW10, TW15 and TW20 glasses.



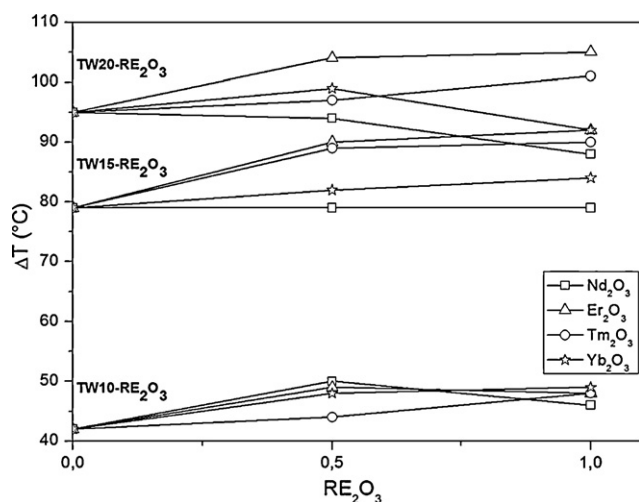


Fig. 6. Effect of rare-earth dopants (Nd<sub>2</sub>O<sub>3</sub>, Er<sub>2</sub>O<sub>3</sub>, Tm<sub>2</sub>O<sub>3</sub>, Yb<sub>2</sub>O<sub>3</sub> mol%) on thermal stability of TW10, TW15 and TW20 glasses.

introducing rare-earth elements into tungsten–tellurite glasses and increasing their content resulted in an increase in glass transition temperatures.

A similar increase in the glass transition temperature was observed in different glass systems with the addition of rare-earth elements [21,27–29]. El-Mallawany and Abbas Ahmed [21] reported that the glass transition temperature significantly increases in quaternary glasses of the form 80TeO<sub>2</sub>–5TiO<sub>2</sub>–(15–x)WO<sub>3</sub>–xA<sub>n</sub>O<sub>m</sub> (A<sub>n</sub>O<sub>m</sub> is Nd<sub>2</sub>O<sub>3</sub> and Er<sub>2</sub>O<sub>3</sub>) with the increasing Nd<sub>2</sub>O<sub>3</sub> and Er<sub>2</sub>O<sub>3</sub> content from 0.01 to 7 mol%. Moreover, it was reported that the increase in glass transition temperature is due to the partial substitution of WO<sub>3</sub> by rare-earth elements of greater number of cations per mol and average cross-linking density. El-Mallawany and Abbas Ahmed [21] also declared that the number of bonds per unit volume increases with the increasing rare-earth element content which leads to an increase in glass transition temperature. Similarly, in the present study the partial substitution of TeO<sub>2</sub> and WO<sub>3</sub> by different rare-earth elements (Nd<sub>2</sub>O<sub>3</sub>, Er<sub>2</sub>O<sub>3</sub>, Tm<sub>2</sub>O<sub>3</sub>, Yb<sub>2</sub>O<sub>3</sub>) showed an increasing effect on glass transition temperature, which is in agreement with the literature.

The temperature difference between  $T_g$  and the first exothermic peak onset  $T_{c1}$ , i.e.  $\Delta T = T_{c1} - T_g$ , indicating a measure for the thermal stability against crystallization were found to be 42, 79 and 95 °C for TW10, TW15 and TW20 samples, respectively (see Fig. 6). For TW10 sample, the addition of 0.5 mol% content of all rare-earth elements slightly increased the thermal stability; however increasing the dopant content did not cause a significant change. For TW15 sample, the addition of Er<sub>2</sub>O<sub>3</sub> and Tm<sub>2</sub>O<sub>3</sub> increased the thermal stability of the glass sample to much higher values than Nd<sub>2</sub>O<sub>3</sub> and Yb<sub>2</sub>O<sub>3</sub>. Increasing the dopant content from 0.5 to 1.0 mol% did not change the thermal stability significantly. For TW20 sample, the addition of 0.5 mol% content of Er<sub>2</sub>O<sub>3</sub> increased the thermal stability to much higher values than Tm<sub>2</sub>O<sub>3</sub> and Yb<sub>2</sub>O<sub>3</sub>, while Nd<sub>2</sub>O<sub>3</sub> addition did not show a change on the thermal stability. By increasing the rare-earth element content from 0.5 to 1.0 mol% in TW20 glass sample, no significant change was observed in the thermal stability for Er<sub>2</sub>O<sub>3</sub> and Tm<sub>2</sub>O<sub>3</sub>, whereas for Nd<sub>2</sub>O<sub>3</sub> and Yb<sub>2</sub>O<sub>3</sub> thermal stability of the glass was significantly decreased. In general, although addition of rare-earth elements to undoped samples and increasing their content resulted in an increase in both glass transition and crystallization temperatures, as the first crystallization onset temperatures ( $T_{c1}$ ) shifted to much higher values than the glass transition temperatures ( $T_g$ ), the  $\Delta T$  values showed

an increase. However, the increase in dopant content from 0.5 to 1.0 mol% did not result in a significant change on the thermal stability of the glasses.

In the literature, generally the thermal stability against crystallization was calculated as the difference between the glass transition onset and the first exothermic peak onset [1,4,6,7,14]. However, El-Mallawany and Abbas Ahmed [21] calculated the thermal stability of the glass samples by subtracting the glass transition onset temperature from the first exothermic peak temperature and reported that the thermal stability range for the glass provides a good estimate of the tendency of the glass to crystallize and should usually be larger than 100 °C to obtain thick glass samples. In the present study, the thermal stability of the glasses were greater than 100 °C when the exothermic peak temperature was taken into account apart from TW10 sample and the thermal stability of the glasses showed an increase with the addition of rare-earth dopants which might increase their use for fiber drawing and planar waveguide fabrication.

#### 4. Conclusions

The effect of rare-earth dopants and different glass preparing techniques on the thermal behavior of tungsten–tellurite glasses were investigated by running detailed differential thermal analyses. Therefore, three different glass samples were prepared with the compositions of (1–x)TeO<sub>2</sub>–xWO<sub>3</sub>, where x=0.10, 0.15 and 0.20 in molar ratio and the samples were doped with 0.5 and 1.0 mol% of Nd<sub>2</sub>O<sub>3</sub>, Er<sub>2</sub>O<sub>3</sub>, Tm<sub>2</sub>O<sub>3</sub> and Yb<sub>2</sub>O<sub>3</sub>. Different melt-quenching techniques used in the experiments showed that different glass preparing methods does not cause a significant change on the thermal behavior. However, the addition of rare-earth elements to undoped samples and increasing their content from 0.5 to 1.0 mol% changed the thermal behavior of the glasses by shifting the glass transition and exothermic reaction temperatures to higher values and increasing the thermal stability. With the introduction of rare-earth dopants, the temperature values of the first endothermic peak corresponding to the eutectic reaction significantly decreased and liquidus reaction temperatures were slightly shifted to lower temperature values. The addition of rare-earth elements with higher atomic number (Er<sub>2</sub>O<sub>3</sub>, Tm<sub>2</sub>O<sub>3</sub> and Yb<sub>2</sub>O<sub>3</sub>) caused the splitting of the first endothermic peak corresponding to the eutectic reaction of the system.

#### Acknowledgement

The authors of this study gratefully acknowledge The Scientific & Technological Research Council of Turkey (TUBITAK) for the financial support under the project numbered 108M077.

#### References

- [1] R.A.H. El-Mallawany, Tellurite Glasses Handbook, CRC Press, Boca Raton, 2002.
- [2] N.N. Smirnova, K.V. Kandevev, A.M. Kut'in, M.F. Churbanov, I.A. Grishin, A.V. Markin, T.A. Bykova, Journal of Inorganic Materials 43 (2007) 1145–1152.
- [3] M.L. Öveçoğlu, G. Özen, S. Cenk, Journal of the European Ceramic Society 26 (2006) 1149–1158.
- [4] S. Blanchandin, P. Marchet, P. Thomas, J.C. Champarnaud-Mesjard, B. Frit, A. Chagraoui, Journal of Materials Science 34 (1999) 4285–4292.
- [5] R. Balda, J. Fernández, J.M. Fernández-Navarro, Optics Express 17 (2009) 8781–8788.
- [6] T. Kosuge, Y. Benino, V. Dimitrov, R. Sato, T. Komatsu, Journal of Non-Crystalline Solids 242 (1998) 154–164.
- [7] I. Shaltout, Y. Tang, R. Braunstein, A.M. Abu-Elazm, Journal of Physics and Chemistry of Solids 56 (1994) 141–150.
- [8] P. Charton, L. Gengembre, P. Armand, Journal of Solid State Chemistry 168 (2002) 175–183.
- [9] D. Lezal, J. Pedlikova, P. Kostka, J. Bludska, M. Poulain, J. Zavadil, Journal of Non-Crystalline Solids 284 (2001) 288–295.
- [10] B. Öz, I. Kabalci, M.L. Öveçoğlu, G. Özen, Journal of the European Ceramic Society 27 (2007) 3239–3251.

- [11] M.J.F. Digonnet, Rare Earth Doped Fiber Lasers and Amplifiers, Dekker, New York, 1993.
- [12] I. Iparraguirre, J. Azkargorta, J.M. Fernandez Navarro, M. Al-Saleh, J. Fernandez, R.J. Balda, Journal of Non-crystalline Solids 353 (2007) 990–992.
- [13] G.N. Wang, S.Q. Xu, J.H. Yang, S.X. Dai, J.J. Zhang, L.L. Hu, Z.Z. Jiang, Chinese Physics Letters 21 (2004) 173–175.
- [14] S. Cenik, B. Demirata, M.L. Öveçoğlu, G. Özen, Spectrochimica Acta 57 (2001) 2367–2372.
- [15] H. Kalaycıoğlu, H. Cankaya, M. Natali Cizmeciyan, A. Sennaroglu, G. Ozen, Journal of Luminescence 128 (2008) 1501–1506.
- [16] G. Özen, A. Aydınli, S. Cenik, A. Sennaroglu, Journal of Luminescence 101 (2003) 293–306.
- [17] S. Zhao, B. Chen, L. Wen, L. Hu, Materials Chemistry and Physics 99 (2006) 210–213.
- [18] E.B. Intyushin, V.A. Novikov, Thin Solid Films 516 (2008) 4194–4200.
- [19] H. Cankaya, A. Sennaroglu, Applied Physics B: Laser and Optics 99 (2010) 121–125.
- [20] H. Kalaycıoğlu, H. Cankaya, G. Ozen, M.L. Ovecoglu, A. Sennaroglu, Optics Communications 281 (2008) 6056–6060.
- [21] R. El-Mallawany, I. Abbas Ahmed, Journal of Materials Science 43 (2008) 5131–5138.
- [22] S. Al-Ani, C.A. Hogarth, R.A. El-Mallawany, Journal of Materials Science 20 (1985) 661–667.
- [23] A.E. Ersundu, M. Çelikkilek, G. Karaduman, N. Solak, S. Aydın, 138th TMS Annual Meeting and Exhibition, vol. 3, San Francisco CA, Supplemental Proceedings, 2009, pp. 709–715.
- [24] M. Çelikkilek, G. Karaduman, A.E. Ersundu, N. Solak, D. Tatar, S. Aydın, 11th International Conference and Exhibition of the European Ceramic Society, Krakow, Poland, 2009.
- [25] A.E. Ersundu, M. Çelikkilek, G. Karaduman, N. Solak, S. Aydın, Phase Studies in the  $\text{TeO}_2\text{--WO}_3$  System, I. International Ceramic, Glass, Procelain, Enamel, Glaze and Pigment Congress–Seres'09, Türkiye, Eskişehir, 2009, pp. 1181–1188.
- [26] V.V. Safonov, Russian Journal of Inorganic Chemistry 53 (2008) 509–511.
- [27] G. Zhang, M.J. Poulain, Journal of Alloys and Compounds 275–277 (1998) 15–20.
- [28] Y. Menke, V. Peltier-Baron, S. Hampshire, Journal of Non-Crystalline Solids 276 (2000) 145–150.
- [29] F. Lofaj, R. Satet, M.J. Hoffman, A.R. Arellano Lopez, Journal of the European Ceramic Society 24 (2004) 3377–3385.